

A New Model Calculation Using Probability for Heat-Assisted Magnetic Recording

T. Kobayashi, F. Inukai, K. Enomoto, and Y. Fujiwara

Graduate School of Engineering, Mie Univ., 1577 Kurimamachiya-cho, Tsu 514-8507, Japan

We propose a new model calculation using the reversal probability of grain magnetization for heat-assisted magnetic recording (HAMR). Our new model calculation can obtain the bit error rate as a function of the writing field H_w for a given anisotropy constant ratio K_u / K_{bulk} , which is a new parameter that we introduced. The physical implication of the recording time window proposed in the micromagnetic calculation is discussed using the new model calculation. Although the recording time window is a good guideline for write-error and erasure-after-write (EAW), EAW cannot be determined solely by the recording time window. The influence of EAW is accurately examined. The allowable range of H_w and K_u / K_{bulk} is also provided for various Curie temperatures T_c . T_c and the heat-transfer thermal gradient are important parameters for reducing K_u / K_{bulk} .

Key words: heat-assisted magnetic recording, model calculation, anisotropy constant ratio, recording time window, Curie temperature, thermal gradient

1. Introduction

Various methods have been proposed with the aim of increasing the areal density of magnetic recording beyond the trilemma limit¹⁾ for granular media. The methods include shingled magnetic recording (SMR), the use of media with a relatively large grain size or bit patterned media (BPM), heat-assisted magnetic recording (HAMR), and microwave-assisted magnetic recording.

It has been reported that the medium thermal stability factor $K_u V / kT$ must exceed 60 to ensure that the grain magnetization direction remains stable during 10 years of archiving, where K_u , V , k , and T are the grain anisotropy constant, the grain volume, the Boltzmann constant, and temperature, respectively. In our previous papers^{2, 3)}, we evaluated the statistical thermal stability factor TSF_{10} corresponding to a value of 60, that is, $K_u V / kT > \text{TSF}_{10}$, and we showed that the minimum K_u value for the stability is reduced by decreasing the grain number per bit (increasing the grain size) since V increases despite the fact that TSF_{10} increases. Furthermore, we also showed that the standard deviation of the dot size for BPM must be restricted to a small value.

We have already reported a HAMR model calculation⁴⁾ using TSF_{10} in order to shorten the calculation time and grasp the physical implications. In that paper, we introduced the anisotropy constant ratio K_u / K_{bulk} as a design guideline. K_u / K_{bulk} is the intrinsic ratio of medium K_u to bulk K_u . We must design a medium with a smaller K_u / K_{bulk} if we are to achieve good media productivity. We have subsequently improved our model calculation by introducing a statistical thermal stability factor during writing, and we revealed the dependence of the minimum K_u / K_{bulk} value on the change of one parameter among many design parameters⁵⁾. As a result, we found that

increasing the writing temperature T_w is only effective for reducing K_u / K_{bulk} . We also provided examination results for a combination of more than two parameters⁶⁾. In conclusion, the combinations that can reduce K_u / K_{bulk} always have SMR as one parameter. However, the use of SMR sometimes degrades the read/write performance of the hard drive. Although a lower T_w is better in terms of the heat resistance of the writing head and/or the surface lubricant, increasing T_w appears to be the only way of reducing K_u / K_{bulk} for HAMR media. Increasing T_w has many advantages in addition to reducing K_u / K_{bulk} ⁷⁾. We have recently improved our model calculation⁸⁾ by introducing the concept of the recording time window⁹⁾ proposed in a micromagnetic simulation. This improvement means the results obtained using the model calculation become consistent with those obtained using the micromagnetic simulation.

In this study, we propose a new HAMR model calculation using the reversal probability of grain magnetization for each attempt. The required statistical thermal stability factor (TSF) is a function of the bit error rate (bER). Therefore, a previous model calculation using TSF can obtain the minimum K_u / K_{bulk} value for a given bER. A new model calculation can obtain the bER as a function of the writing field H_w for a given K_u / K_{bulk} . We discuss the physical implication of the recording time window using a new model calculation. The allowable ranges of H_w and K_u / K_{bulk} are also provided for various Curie temperatures.

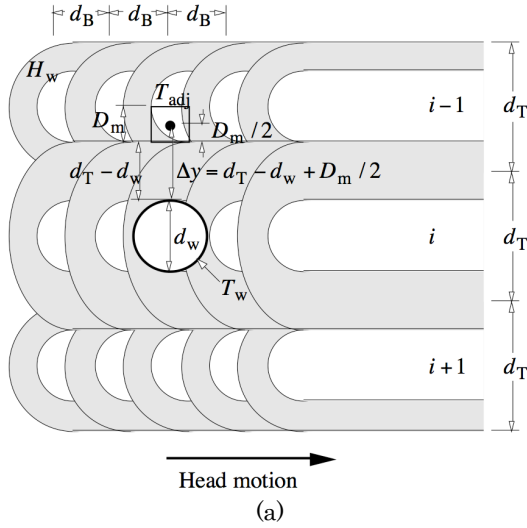
2. Calculation Conditions

2.1 Recording conditions

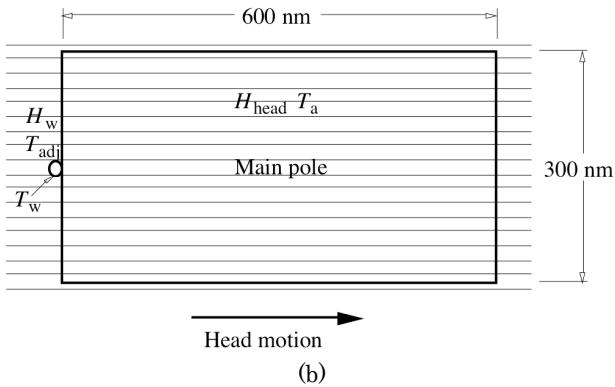
The medium was assumed to be granular. The arrangement of the grains was not considered. Figure 1 (a) is a schematic illustration of the area near the writing position for HAMR. The writing field H_w is

applied to a wide area including the writing position. The circle denoted the writing temperature T_w is an isotherm of T_w , and d_w is the heat-spot diameter. T_w is defined in 3.1. The white regions indicate upward or downward magnetization, and the gray regions indicate a magnetization transition that contains upward and downward magnetization grains. The transition region spreads to adjacent tracks as a result of rewriting operations on the i th track. T_{adj} is the maximum temperature at which information in adjacent tracks can be held during rewriting. Δy is the distance between T_w and T_{adj} , and was assumed to be $d_T - d_w + D_m/2$, where d_T is the track pitch and D_m is the mean grain size. d_B is the bit pitch.

Figure 1 (b) shows the writing-head configuration. We assume that the main-pole size of the head is 600 nm (down-track direction) \times 300 nm (cross-track direction), and the writing position is located on the trailing side of the main pole. H_{head} is the maximum head field that can hold information under the main pole during rewriting. The maximum temperature under the main pole is T_a , which is the maximum ambient temperature of the hard drive, and is assumed to be 330 K.



(a)



(b)

Fig. 1 Schematic illustrations of (a) writing position and (b) writing-head configuration.

Table 1 Recording parameters and standard values.

User areal density (Tbps)	4
Bit area $S = d_B \times d_T$ (nm ²)	140
Bit aspect ratio d_T/d_B	3
Heat-spot diameter d_w	$d_T/2$
Ambient temperature T_a (K)	330
Linear velocity v (m/s)	10

The recording parameters and the standard values are summarized in Table 1. The areal density calculated from the bit area S is 0.6 Tbps larger than the user areal density. The difference is the data for the error correction code and others.

$d_w = d_T/2$ is a design parameter, and is changed by the light power used for heating. If the light power alone is increased for a medium with the same Curie temperature T_c , the temperature profile increases and the written bits will be spread in the cross-track direction. Thus it becomes impossible to keep the track pitch constant. Therefore, we must adjust T_c to maintain d_w when we change the temperature profile by changing the light power.

2.2 Medium conditions

The standard medium structure is shown in Fig. 2. The standard medium consists of four layers, that is, a recording layer RL (Fe-Pt base, thickness $h = 8$ nm), an interlayer 1 IL1 (MgO base, 5 nm), an interlayer 2 IL2 (Cr base, 10 nm), and a heat-sink layer HSL (Cu base, 30 nm). The x , y , and z axes are the down-track, cross-track, and thickness directions, respectively. d_w is defined at the heat-spot edge and is at the center of the RL layer in the thickness direction. The two positions of T_w in Fig. 2 are at a distance of d_w in the cross-track direction as shown in Fig. 1 (a).

The medium parameters and the standard values are summarized in Table 2. D_m can be calculated from $\sqrt{S/n} - \Delta$, where n is the grain number per bit and Δ is the non-magnetic spacing between grains. K_{um} is the mean anisotropy constant. The standard deviation of the Curie temperature σ_{T_c} is assumed to be zero.

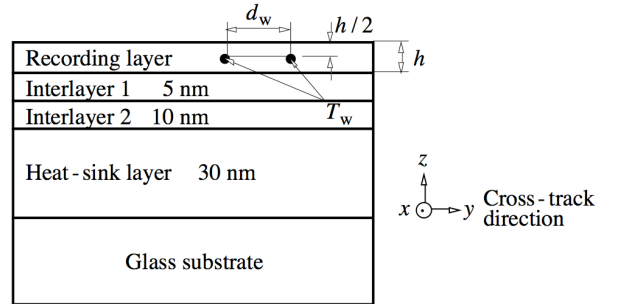


Fig. 2 Standard medium structure and definition of writing temperature T_w .

Table 2 Medium parameters and standard values.

RL thickness h (nm)	8
Non-magnetic spacing Δ (nm)	1
Grain number per bit n (grain/bit)	4
Standard deviation of grain size σ_D/D_m (%)	10
Standard deviation of anisotropy σ_K/K_{um} (%)	0
Standard deviation of Curie temp. σ_{T_c}/T_c (%)	0

The temperature dependence of the magnetization M_s was determined using a mean field analysis⁴⁾, and that of K_{um} was assumed to be proportional to M_s^2 . T_c can be adjusted by the Cu simple dilution of $(Fe_{0.5}Pt_{0.5})_{1-z}Cu_z$. $M_s(T_c, T)$ is a function of T_c and T , and $M_s(T_c = 770 \text{ K}, T = 300 \text{ K}) = 1000 \text{ emu/cm}^3$ was assumed. On the other hand, $K_{um}(T_c, K_u/K_{bulk}, T)$ is a function of T_c , K_u/K_{bulk} , and T , and $K_{um}(T_c = 770 \text{ K}, K_u/K_{bulk} = 1, T = 300 \text{ K}) = 70 \text{ Merg/cm}^3$ was assumed. K_u/K_{bulk} is the intrinsic ratio of medium K_u to bulk K_u . It is necessary to design a medium with a smaller K_u/K_{bulk} in terms of achieving good media productivity.

2.3 Heat-transfer calculation conditions

The heat-transfer calculation conditions including the thermal conductivities for each layer are the same as those reported in a previous paper⁴⁾.

The heat-transfer thermal gradients $\partial T/\partial x$ for the down-track direction and $\partial T/\partial y$ for the cross-track direction are calculated by a heat-transfer simulation. $\partial T/\partial x$ and $\partial T/\partial y$ for $T_w = T_{wj}$ can be calculated using those for $T_w = T_{wi}$ as

$$\frac{\partial T}{\partial x}(T_{wj}) = \frac{\partial T}{\partial x}(T_{wi}) \frac{T_{wj} - T_a}{T_{wi} - T_a} \quad \text{and} \quad (1)$$

$$\frac{\partial T}{\partial y}(T_{wj}) = \frac{\partial T}{\partial y}(T_{wi}) \frac{T_{wj} - T_a}{T_{wi} - T_a}, \quad (2)$$

respectively. Equations (1) and (2) are valid for T_c instead of T_w since $T_w \approx T_c$. It is important that the heat-transfer thermal gradient is simultaneously increased as T_w (T_c) increases. Since $\partial T/\partial x \approx \partial T/\partial y$, $\partial T/\partial x = \partial T/\partial y$ is expressed as $\partial T/\partial x(y)$ in the following.

Table 3 Bit error rate calculation parameters and standard values.

Attempt frequency f_0 (s^{-1})	10^{11}
(Attempt period τ_{AP} (ns))	0.01
Maximum rewriting number N_{rew}	10^4
Signal threshold	0.35
Bit error rate bER	10^{-3}

2.4 Bit error rate calculation conditions

The bit error rate (bER) calculation parameters and the standard values are summarized in Table 3.

The statistical thermal stability factor TSF is calculated statistically using many bits. Each bit has n grains, and the grains have various sizes D and anisotropy constants K_u . D (lognormal distribution) and K_u (normal distribution) are randomly generated by a computer. Each grain has the grain error probability P

$$P = 1 - \exp\left(-f_0\tau \exp\left(-\text{TSF} \cdot \left(\frac{D}{D_m}\right)^2 \cdot \frac{K_u}{K_{um}}\right)\right), \quad (3)$$

where τ is time. TSF is the thermal stability factor for $D = D_m$ and $K_u = K_{um}$, and is unrelated to K_u . The bER is a function of $P(\tau, \text{TSF})$, n , σ_D , and σ_K . If the bER is fixed, TSF is a function of τ , n , σ_D , and σ_K , that is, $\text{TSF}(\tau, n, \sigma_D, \sigma_K)^{2, 3)}$.

Errors occur in some grains of a bit. It is assumed that if the sum of the area with no error grains $\sum D_i^2$ is 35 % larger than nD_m^2 in one bit, the bit has no error. The maximum allowable bER is assumed to be 10^{-3} .

3. Calculation Method

3.1 Reversal probability of grain magnetization

First, we explain the reversal probability of grain magnetization and the recording time window. The magnetization reversal number during τ is given by

$$f_0\tau \exp(-K_\beta), \quad (4)$$

where K_β is the medium thermal stability factor. When $\tau = \tau_{AP} = 1/f_0 = 10^{-11} \text{ s} = 0.01 \text{ ns}$, Eq. (4) becomes

$$\exp(-K_\beta), \quad (5)$$

where τ_{AP} is the attempt period. Equation (5) is the reversal probability of grain magnetization for each attempt. For example, when $K_\beta = 0$, $\exp(-K_\beta)$ becomes one, where M_s reversal always occurs for each attempt. $K_{\beta+}$ where M_s is parallel to the writing field H_w , and $K_{\beta-}$ where M_s is antiparallel to H_w are expressed by

$$K_{\beta+}(T, H_w) = \frac{K_u(T)V}{kT} \left(1 + \frac{H_w}{H_c(T)}\right)^2, \quad (6)$$

and

$$K_{\beta-}(T, H_w) = \frac{K_u(T)V}{kT} \left(1 - \frac{H_w}{H_c(T)}\right)^2 \quad (H_w \leq H_c(T)),$$

$$K_{\beta-}(T, H_w) = 0 \quad (H_c(T) < H_w), \quad (7)$$

respectively, where H_c is the coercivity. Therefore, the probability p_+ for each attempt where M_s and H_w change from parallel to antiparallel is expressed by

$$p_+ = \exp(-K_{\beta+}). \quad (8)$$

On the other hand,

$$p_- = \exp(-K_{\beta-}) \quad (9)$$

is the probability for each attempt where M_s and H_w change from antiparallel to parallel.

In this paper, the recording time window τ_{RW} is defined by

$$\tau_{RW} = \frac{T_c - T_w}{(\partial T / \partial x) \cdot v}, \quad (10)$$

where v is the linear velocity. Since $v = \partial x / \partial t$, $(\partial T / \partial x) \cdot v$ is the cooling rate $\partial T / \partial t$. Therefore, τ_{RW} is the cooling time from T_c to T_w . And then, the relationship between H_w and T_w is defined by

$$\begin{aligned} H_w &= H_{cm}(T_c, K_u / K_{bulk}, T_w) \\ &= \frac{2K_{um}(T_c, K_u / K_{bulk}, T_w)}{M_s(T_c, T_w)}, \end{aligned} \quad (11)$$

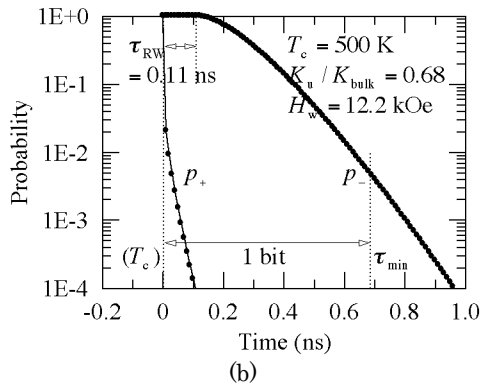
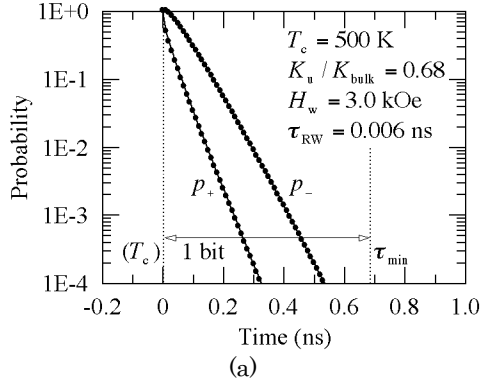


Fig. 3 Dependence of reversal probability of grain magnetization on time for (a) writing field $H_w = 3.0$ kOe and (b) 12.2 kOe.

where H_{cm} is the mean coercivity. The media can be designated by T_c and K_u / K_{bulk} . On the other hand, τ_{RW} is a function of T_c , K_u / K_{bulk} , $\partial T / \partial x$, v and H_w since T_w is a function of T_c , K_u / K_{bulk} and H_w .

Figure 3 shows the dependence of the reversal probability of grain magnetization on time. The time corresponding to T_c is 0 ns, and the minimum magnetization transition window $\tau_{min} = d_B / v$ corresponding to 1 bit is 0.68 ns since d_B is 6.8 nm and v is 10 m/s. The time after τ_{min} corresponds to the next bit. The filled circles are the probabilities for each attempt. The p_+ and p_- values are both one at 0 ns since $K_{\beta\pm} = 0$. p_- is always equal to one during τ_{RW} . A lower p_+ and a higher p_- are better between 0 and τ_{min} in terms of stable writing, and lower p_+ and p_- values are both better after τ_{min} in terms of information (written bit) stability.

Figure 3 (a) shows the result when $T_c = 500$ K, $K_u / K_{bulk} = 0.68$ and H_w is low ($= 3.0$ kOe). The resulting τ_{RW} value is 0.006 ns, and τ_{RW} is too short. p_- is rapidly decreased after 0 ns and p_+ is not sufficiently low before τ_{min} , which is not suitable for stable writing. This corresponds to write-error (WE).

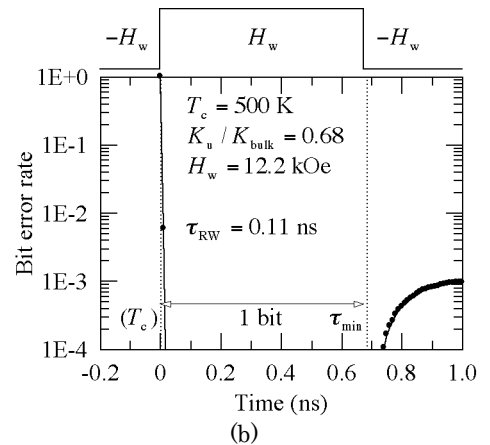
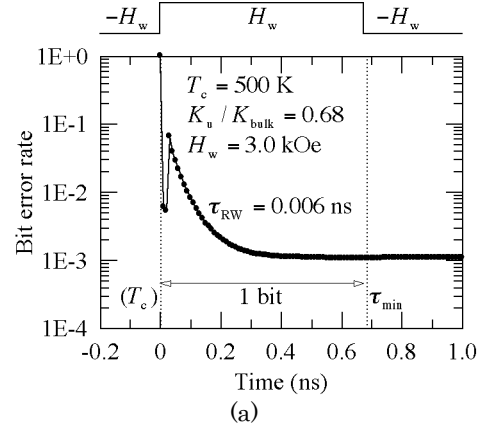


Fig. 4 Dependence of bit error rate on time for (a) writing field $H_w = 3.0$ kOe and (b) 12.2 kOe.

Figure 3 (b) shows the result when $T_c = 500$ K, $K_u / K_{bulk} = 0.68$ and H_w is high ($= 12.2$ kOe). The

resulting τ_{RW} value is 0.11 ns, and τ_{RW} is too long. In this case, p_- is sufficiently high and p_+ is sufficiently low before τ_{RW} . Therefore, low WE can be expected. However, p_- has a relatively large value after τ_{min} corresponding to the next bit, which is unsuitable as regards the information stability at the next bit when the direction of H_w is changed after τ_{min} . This corresponds to erasure-after-write (EAW).

3.2 Bit error rate calculation

The bER can be calculated by the Monte Carlo method using the reversal probability of grain magnetization p_{\pm} for each attempt period. First, the medium is determined by T_c and K_u/K_{bulk} . The grain temperature falls from T_c according to $\partial T/\partial x$ and v during the writing process. The magnetic property and then p_{\pm} are calculated by employing a mean field analysis for each attempt period. The magnetization direction can be determined by the Monte Carlo method for each attempt period. The bER is obtained from the mean of 10^6 bits since the results are scattered.

Figure 4 (a) shows the bER dependence on time for the same conditions shown in Fig. 3 (a). The direction of H_w is changed after τ_{min} to examine the EAW. The bER remains high before τ_{min} since H_w is too low, that is, WE. A case where H_w is too high is shown in Fig. 4 (b), which corresponds to Fig. 3 (b). Although the bER is sufficiently low before τ_{min} , it increases after τ_{min} , that is, EAW.

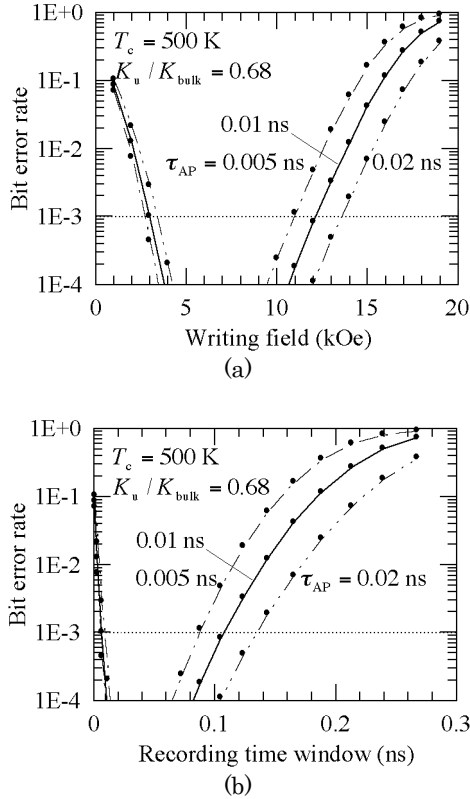


Fig. 5 Dependence of bit error rate on (a) writing field and (b) recording time window for various attempt periods τ_{AP} .

3.3 Attempt period

The attempt period is an uncertain parameter. Figure 5 shows the bER dependence on (a) H_w and (b) τ_{RW} for various attempt periods τ_{AP} . A high bER in a low H_w (a short τ_{RW}) range is caused by WE, and that in a high H_w (a long τ_{RW}) range is caused by EAW. The overall tendencies of bER are not greatly changed by doubling τ_{AP} .

3.4 HAMR conditions

Five HAMR conditions are examined to estimate the allowable ranges of H_w and K_u/K_{bulk} .

Condition I is the information stability during 10 years of archiving. The minimum K_u/K_{bulk} value can be calculated using a previous model calculation⁴⁾ by solving

$$\frac{K_{um}(T_c, K_u/K_{bulk}, T_a)V_m}{kT_a} = \text{TSF}_{10} \equiv \text{TSF}(10 \text{ years}, n, \sigma_D, \sigma_K), \quad (12)$$

where V_m is the grain volume for mean grain size.

Condition II is the restriction of WE. The minimum H_w value for WE can be calculated using the new model calculation mentioned in 3.2.

Condition III is the restriction of EAW. The maximum H_w value for EAW can also be calculated using the new model calculation mentioned in 3.2.

Condition IV is the information stability in adjacent tracks during rewriting, that is, adjacent-track-interference (ATI). The maximum H_w value for ATI can be calculated by solving

$$K_{\beta-}(T_{adj}, H_w) = \text{TSF}_{adj} \equiv \text{TSF}\left(\frac{d_B}{v} \times N_{rew}, n, \sigma_D, \sigma_K\right) \quad (13)$$

(thermal stability condition)⁵⁾,

$$\frac{T_w(H_w) - T_{adj}}{\Delta y} = \frac{\partial T}{\partial y} \quad (14)$$

(thermal gradient condition)⁵⁾, and Eq. (11).

Condition V is the information stability under the main pole during rewriting. The maximum H_{head} value can be calculated using a previous model calculation⁵⁾ by

$$H_{head} = H_{cm}(T_a) \left(1 - \sqrt{\frac{\text{TSF}_{head}}{K_{um}(T_a)V_m/(kT_a)}}\right), \quad (15)$$

where

$$\text{TSF}_{head} \equiv \text{TSF}(\tau_{head} \times N_{rew} \times (N_T - 1), n, \sigma_D, \sigma_K), \quad (16)$$

$\tau_{head} = 600 \text{ nm}/v$, and $N_T = 300 \text{ nm}/d_T$.

4. Calculation Results

4.1 Heat-transfer thermal gradient

τ_{RW} is a function of T_c , K_u/K_{bulk} , $\partial T/\partial x$, v and H_w . First, we examine the relationship between τ_{RW} and $\partial T/\partial x$. Figure 6 shows the dependence of bER on (a) H_w and (b) τ_{RW} for various $\partial T/\partial x$ values. Open circles indicate the bER for EAW when $\tau_{RW} = 0.1$ ns. As shown in Fig. 6 (b), although the bER values for WE in a short τ_{RW} range (< 0.02 ns) are almost the same for various $\partial T/\partial x$ values, the bER for EAW at $\tau_{RW} = 0.1$ ns for $\partial T/\partial x = 4.9$ K/nm is higher than that for 6.9 K/nm.

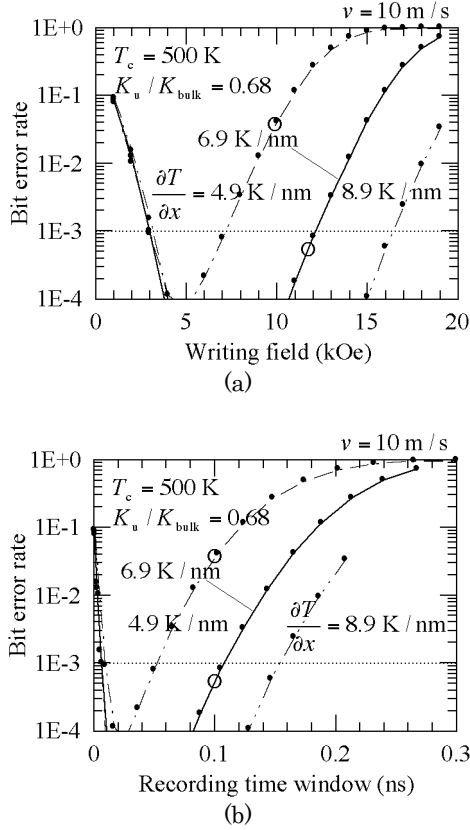


Fig. 6 Dependence of bit error rate on (a) writing field and (b) recording time window for various heat-transfer thermal gradients $\partial T/\partial x$.

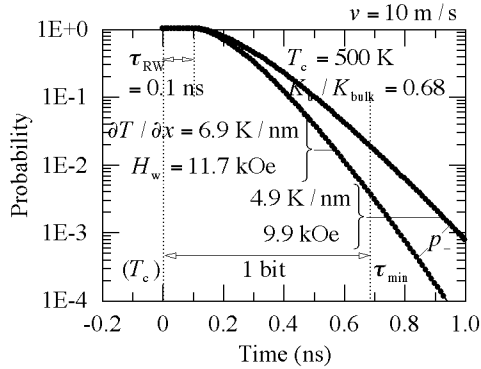


Fig. 7 Dependence of reversal probability of grain magnetization on time for heat-transfer thermal gradients $\partial T/\partial x = 4.9$ K/nm and 8.9 K/nm.

This difference can be explained using Fig. 7. The bER for EAW is determined by p_- after τ_{min} . Although the τ_{RW} values are the same, the p_- values after τ_{min} are different since the $\partial T/\partial x$ values are different. Although τ_{RW} is a good guideline for WE and EAW when $\partial T/\partial x$ is constant as shown in Figs. 3 and 4, EAW cannot be determined solely by τ_{RW} as shown in Figs. 6 and 7 when $\partial T/\partial x$ changes.

4.2 Linear velocity

Next, we examine the relationship between τ_{RW} and v . Figure 8 shows the dependence of bER on (a) H_w and (b) τ_{RW} for various v values. Open circles also indicate the bER for EAW when $\tau_{RW} = 0.1$ ns. The bER at $\tau_{RW} = 0.1$ ns for $v = 20$ m/s is higher than that for 10 m/s as shown in Fig. 8 (b). This difference can be explained using Fig. 9. Since Fig. 9 (a) and (b) show the case where $v = 10$ m/s and 20 m/s, respectively, the τ_{min} values are 0.68 ns and 0.34 ns for Fig. 9 (a) and (b), respectively. The bER for EAW is determined by p_- after τ_{min} . Since the ratios of τ_{RW} to τ_{min} are 14.6 % and 29.3 % for Fig. 9 (a) and (b), respectively, the p_- value after τ_{min} for $v = 20$ m/s is higher than that for $v = 10$ m/s. Therefore, the bER for EAW at $\tau_{RW} = 0.1$ ns for $v = 20$ m/s becomes higher than that for $v = 10$ m/s. EAW cannot be determined solely by τ_{RW} as shown in Figs. 8 and 9 when v changes.

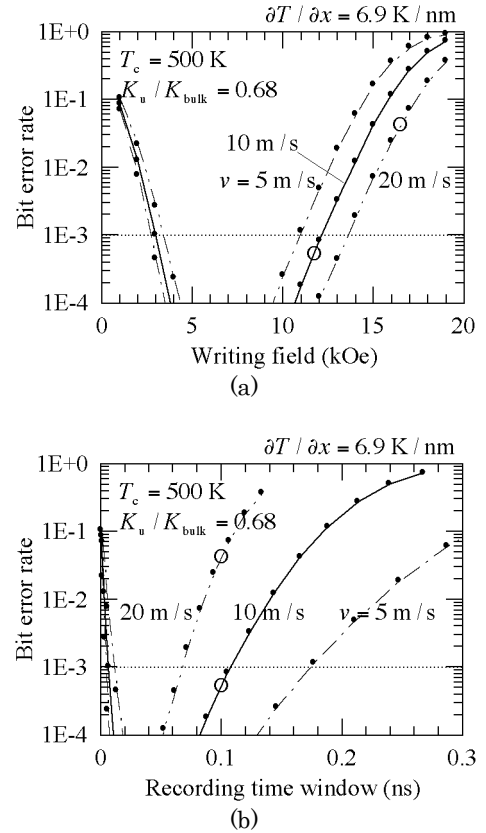


Fig. 8 Dependence of bit error rate on (a) writing field and (b) recording time window for various linear velocities v .

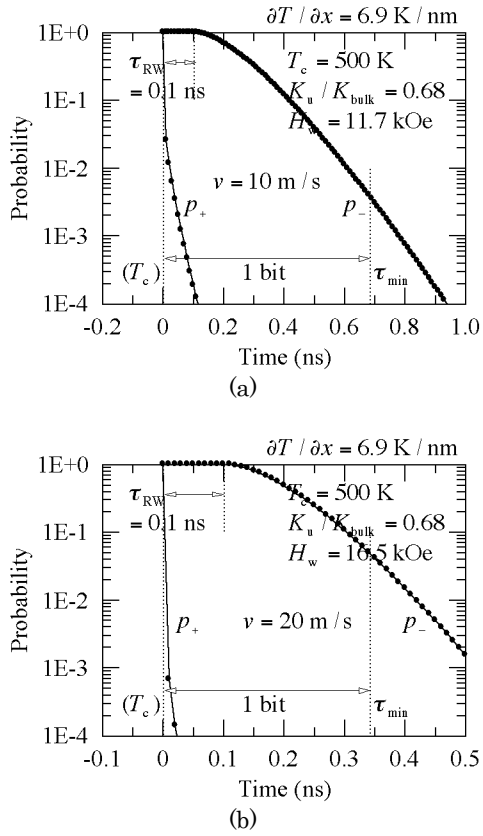


Fig. 9 Dependence of reversal probability of grain magnetization on time for (a) linear velocities $v = 10 \text{ m/s}$ and (b) 20 m/s .

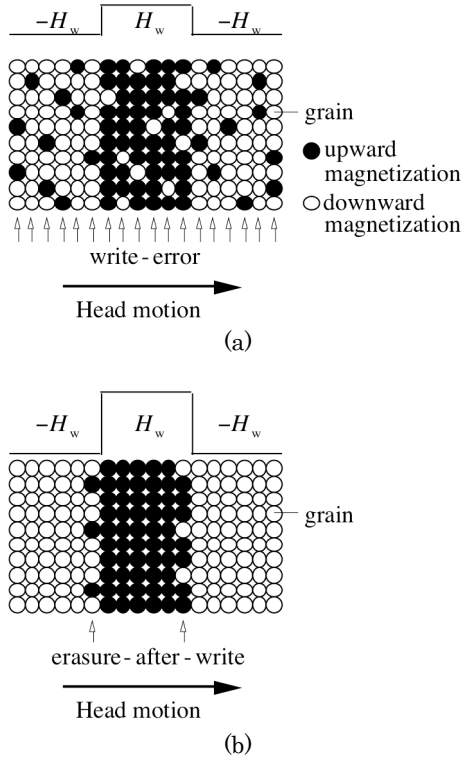


Fig. 10 Schematic illustrations of (a) write-error and (b) erasure-after-write.

Figure 10 shows a schematic illustration of (a) WE and (b) EAW where the bit and the track pitches are much longer than those of this calculation. WE occurs in every grain column during writing as shown in Fig. 10 (a) considering Fig. 4 (a) when H_w is too low. On the other hand, EAW occurs at one or two columns of grains on just the former bit edge as shown in Fig. 10 (b) considering Fig. 4 (b) when H_w is too high. Although WE is independent of bit pitch, the influence of EAW depends on bit pitch, and when the bit pitch is long, it is difficult to examine the influence of EAW. Since the bit pitch is short in this calculation, the influence of EAW can be accurately examined, and EAW will be important for the density of 4 Tbps.

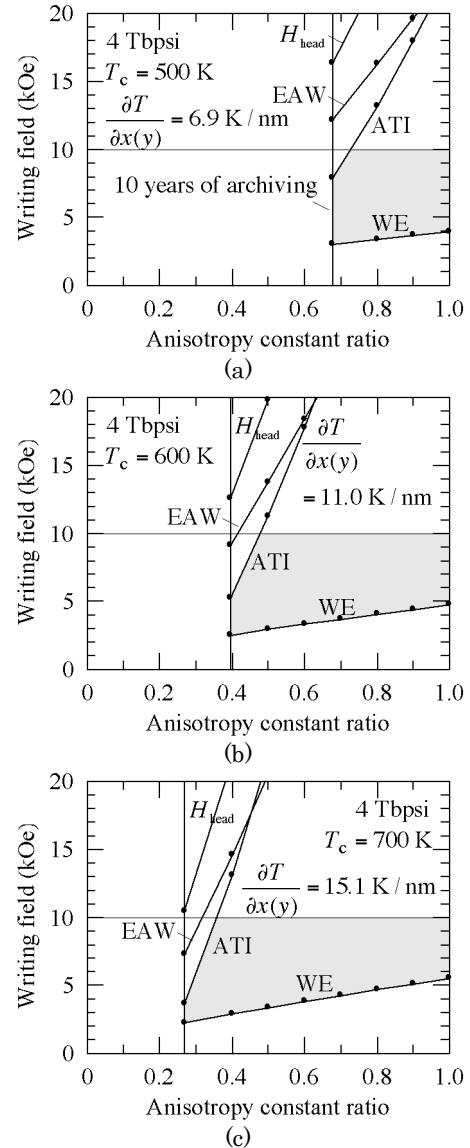


Fig. 11 Allowable range of writing field and anisotropy constant ratio for (a) Curie temperatures $T_c = 500 \text{ K}$, (b) 600 K , and (c) 700 K where WE, EAW, ATI, and H_{head} are write-error, erasure-after-write, adjacent-track-interference, and the maximum head field under the main pole, respectively.

4.3 Allowable range

This model calculation can estimate the allowable range of H_w and K_u/K_{bulk} .

In Fig. 11, condition I (10 years of archiving) determines the minimum K_u/K_{bulk} value, and condition II (WE) determines the minimum H_w value. The maximum H_w value is determined from condition III (EAW), condition IV (ATI), and condition V (H_{head}) as mentioned in 3.4. The maximum H_w value that the writing head can supply was assumed to be 10 kOe. As a result, the gray regions indicate the allowable range. The limiting factors are 10 years of archiving, WE, and ATI in this calculation.

$\partial T/\partial x(y)$ is simultaneously increased as T_c increases in Fig. 11 (a), (b), and (c) as mentioned in 2.3. The minimum K_u/K_{bulk} value (10 years of archiving) becomes low as T_c increases, and then the allowable range widens as T_c increases.

The reason for the shift of the minimum K_u/K_{bulk} value (10 years of archiving) can be explained using the temperature dependence of K_{um} as shown in Fig. 12 where the K_u/K_{bulk} values are the same. The rates at which K_u increase ($\partial K_u/\partial T$) are almost the same. K_{um} at T_a for $T_c = 500$ K is insufficient for 10 years of archiving since the temperature difference between T_c and T_a is small. On the other hand, K_{um} at T_a for $T_c = 700$ K is sufficient. Therefore, the small K_u/K_{bulk} value becomes allowable as T_c increases.

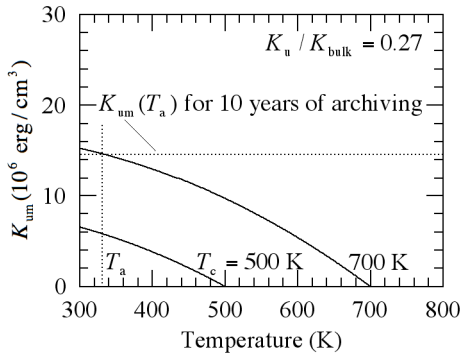


Fig. 12 Dependence of mean anisotropy constant K_{um} on temperature for Curie temperatures $T_c = 500$ K and 700 K.

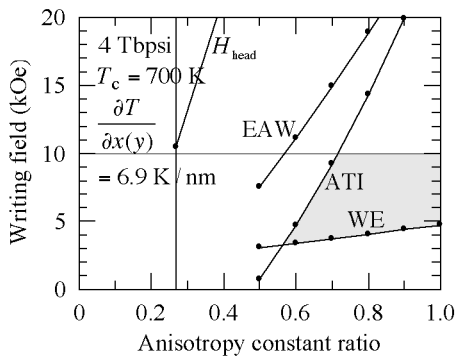


Fig. 13 Allowable range of writing field and anisotropy constant ratio for Curie temperature $T_c = 700$ K and heat-transfer thermal gradient $\partial T/\partial x(y) = 6.9$ K/nm.

Another reason for widening the allowable range is the increase in $\partial T/\partial x(y)$, that is, $\partial T/\partial x(y)$ is simultaneously increased as T_c increases as mentioned in 2.3. Figure 13 shows the allowable range for $T_c = 700$ K when $\partial T/\partial x(y)$ is 6.9 K/nm instead of 15.1 K/nm (Fig. 11 (c)). The maximum H_w value restricted by EAW and ATI, which are closely related to $\partial T/\partial x(y)$, is greatly decreased from Fig. 11 (c). If $\partial T/\partial x(y)$ is not simultaneously increased, the overall tendency of the allowable range is not greatly changed by increasing T_c when we compare Fig. 11 (a) and Fig. 13.

Figure 14 shows the allowable range calculated using the thermal conductivity of interlayer 1 $\kappa_{\text{IL1}} = 0.04$ W/(cmK) reported for sputtered MgO film¹⁰⁾ instead of the standard value of 0.5 W/(cmK)⁴⁾. $\partial T/\partial x(y)$ is decreased from 6.9 K/nm (Fig. 11 (a)) to 5.3 K/nm (Fig. 14 (a)) for $T_c = 500$ K. Then, the allowable range is greatly decreased. Since the allowable range is sensitive to $\partial T/\partial x(y)$, the thermal conductivity is an important design parameter.

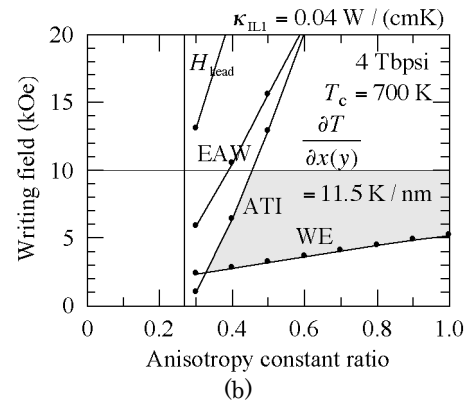
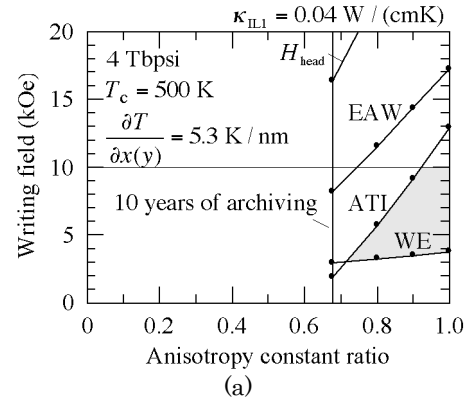


Fig. 14 Allowable range of writing field and anisotropy constant ratio for (a) Curie temperatures $T_c = 500$ K and (b) 700 K when the thermal conductivity of interlayer 1 κ_{IL1} is 0.04 W/(cmK).

5. Conclusions

We propose a new model calculation using the reversal probability of grain magnetization for heat-assisted magnetic recording. The physical implication of the recording time window τ_{RW}

proposed in the micromagnetic calculation is discussed using a new model calculation. Although τ_{RW} is a good guideline for write-error and erasure-after-write (EAW), EAW cannot be determined solely by τ_{RW} . The influence of EAW is accurately examined, and EAW will be important for the density of 4 Tbps.

The allowable range of the writing field and the anisotropy constant ratio K_u/K_{bulk} is also provided for various Curie temperatures T_c . The allowable range widens as T_c increases. The reasons for this are the temperature difference between T_c and the ambient temperature, and the simultaneous increase in the heat-transfer thermal gradient $\partial T/\partial x(y)$ as T_c increases. T_c and $\partial T/\partial x(y)$ are important parameters for reducing K_u/K_{bulk} .

Acknowledgements We acknowledge the support of the Advanced Storage Research Consortium (ASRC), Japan.

References

- 1) S. H. Charap, P. -L. Lu, and Y. He: *IEEE Trans. Magn.*, **33**, 978 (1997).
- 2) T. Kobayashi, T. Kitayama, and Y. Fujiwara: *J. Magn. Soc. Jpn.*, **36**, 282 (2012).
- 3) Y. Isowaki, T. Kobayashi, and Y. Fujiwara: *J. Magn. Soc. Jpn.*, **38**, 1 (2014).
- 4) T. Kobayashi, Y. Isowaki, and Y. Fujiwara: *J. Magn. Soc. Jpn.*, **39**, 8 (2015).
- 5) T. Kobayashi, Y. Isowaki, and Y. Fujiwara: *J. Magn. Soc. Jpn.*, **39**, 139 (2015).
- 6) T. Kobayashi, Y. Isowaki, and Y. Fujiwara: *J. Magn. Soc. Jpn.*, **40**, 1 (2016).
- 7) T. Kobayashi, Y. Isowaki, and Y. Fujiwara: *J. Magn. Soc. Jpn.*, **40**, 28 (2016).
- 8) T. Kobayashi and Y. Fujiwara: *J. Magn. Soc. Jpn.*, **40**, 81 (2016).
- 9) J. -G. Zhu and H. Li: *IEEE Trans. Magn.*, **49**, 765 (2013).
- 10) S. -M. Lee, D. G. Cahill, and T. H. Allen: *Phys. Rev. B*, **52**, 253 (1995).

Received Mar. 31, 2016; Accepted Nov. 7, 2016